Final Draft

of the original manuscript:

Lozano, G.A.; Bellosta von Colbe, J.M.; Bormann, R.; Klassen, T.;
Dornheim, M.:

Enhanced volumetric hydrogen density in sodium alanate by compaction

In: Journal of Power Sources (2011) Elsevier

DOI: 10.1016/j.jpowsour.2011.07.053

Enhanced volumetric hydrogen density in sodium alanate by compaction

Gustavo A. Lozano*, Jose M. Bellosta von Colbe, Rüdiger Bormann, Thomas Klassen, Martin Dornheim

Institute of Materials Research, Materials Technology, Helmholtz-Zentrum Geesthacht, D-21502 Geesthacht, Germany

Abstract

Powder compaction is a potential process for the enhancement of the volumetric and gravimetric capacities of hydrogen storage systems based on metal hydrides. This paper presents the hydrogen absorption and desorption behaviour of compacts of sodium alanate material prepared under different levels of compaction pressure. It is shown that even at high compaction levels and low initial porosities, hydrogen absorption and desorption kinetics can proceed comparatively fast in compacted material. Furthermore, experimental hydrogen weight capacities of compacted material are higher than the experimental values obtained in case of loose powder. It is demonstrated that the kinetic behaviour of the compacted material during cycling is directly associated to the volumetric expansion of the compact, which is quantitatively measured and analyzed during both hydrogen absorption and desorption processes. The cycling behaviour and dimensional changes of compacted sodium alanate material are a key consideration point if it is used as hydrogen storage materials in practical tank systems.

1 Introduction

Among hydrogen storage alternatives, the major advantage of metal hydrides is the larger volumetric hydrogen density. For instance, the complex ternary hydride Mg_2FeH_6 has the highest known hydrogen volumetric density, 150 kg H_2 m^{-3} [1], which is more than twice the density of liquid hydrogen and three times that of hydrogen gas under 700 bar [2]. However, if handled as a loose

* Corresponding author Tel.: +49 41 5287 2643; fax: +49 41 5287 2625. E-mail address: gustavo.lozano@hzg.de, gusaloz@yahoo.com (G.A. Lozano).

powder bed, the effective volumetric hydrogen density of metal hydrides diminishes because of the void volume inside the bed. For instance, loose sodium alanate material has an experimental porosity of more than 60 % (experimental measured density of the alanate bed is 0.6 g ml^{-1} while the solid density of desorbed initial material is 1.8 g ml^{-1}), i.e. the material occupies less than half of the volume of the bed. Fortunately, the effective volumetric hydrogen density in a metal hydride bed can be enhanced by powder densification, i.e. compaction of the material.

In earlier works, the advantages of the compaction of metal hydrides were shown in the cases of $LaNi_5$ [3-5], $LmNi_{4.85}Sn_{0.15}$ [6, 7], $CaNi_5$ [8], TiH_2 [9], MgH_2 [10-12], and $Mg_{90}Ni_{10}$ [13, 14]. They showed that handling metal hydrides as compacts offer several advantages over handling as loose powder in a hydride bed:

- Increased volumetric hydrogen density
- Easier handling
- Improvement of the effective thermal conductivity.

Nevertheless, compacted material has higher heat release/consumption per unit of volume during the hydrogen absorption/desorption process, and its lower porosity may lead to higher resistance to hydrogen flow.

In recent years, research has been focused on light-weight complex hydrides, which also have an even high hydrogen capacity by weight, e.g. $LiBH_4$ [15], $LiBH_4/MgH_2$ [16, 17]. However, these systems still require high operating temperatures for the absorption/desorption process. For the present work, sodium alanate has been selected as scale-up model material to understand and manage possible hurdles in the development of storage systems based on light weight metal hydrides. Sodium alanate, $NaAlH_4$, is reversibly formed in a two-step reaction from NaH and Al within the technically favourable range of up to 125 °C, Eq. 1 and 2 [18].

$$3NaH + Al + 1.5H_2 \xleftrightarrow{cat} Na_3AlH_6 \quad (1)$$

$$Na_3AlH_6 + 2Al + 3H_2 \xleftrightarrow{cat} 3NaAlH_4 \quad (2)$$

It has a theoretical gravimetric hydrogen storage capacity of 5.6 wt%, enabling possible higher gravimetric capacities in comparison to conventional room-temperature metal hydrides. The group of compounds taking part in these equations, which is sometimes also called Na-Al-H system, will be referred in this investigation as sodium alanate material.

Motivated by the potential advantages of metal hydride compaction on the performance of practical storage systems, this paper presents and analyses the hydrogen sorption properties of compacts of sodium alanate material. In addition to the cycling effects on the sorption behaviour, the compaction level in the material preparation is considered. Special emphasis is given to dimensional and morphology changes of the compacts during cycling. Both cycling behaviour and dimensional changes

of the compacts are key features in the implementation of compacted metal hydrides in practical applications.

2 Experimental procedures

Sodium alanate material in the desorbed state was used for the compacts manufacture. The material was prepared by high energy ball milling as explained in previous works [19, 20]. Accounting the addition of inert material (2 mol% aluminium-reduced $TiCl_4$ as catalyst precursor), the maximal hydrogen capacity of the material is 5.0 wt%. All handling was carried out inside a glove box under purified argon atmosphere.

The milled material, initially a loose powder, was uniaxial compacted and shaped into cylindrical moulds of 4 and 8 mm diameter, using a hydraulic axial press. The hydraulic press was composed of a single acting cylinder with a capacity of 5 ton-force and a hydraulic hand pump with a maximal pressure of 700 bar. The height of the compacts varied from 2 to 3 mm for the 4-mm diameter compacts, and from 5 to 6 mm for the 8-mm diameter compacts. The compaction pressure was gradually varied from compact to compact, such that different apparent densities and porosities were obtained. Compaction pressures up to 2.1 GPa were applied. The compaction procedure began by filling the loose powder material in the cavity of the mould. Afterwards, the material was compacted under the desired level of pressure for two minutes. The pressure was subsequently released for a minute. A second consolidation was performed at the same level of compaction pressure for another 2 minutes and the compact was then finally ejected out of the mould.

Sorption kinetics of compacts manufactured under different compaction pressures was characterized using a Sieverts' type apparatus (HERA, Quebec, Canada) that works based on a pressure-volumetric method combined with differential-pressure measurements [21]. The standard conditions applied in all sorption kinetics measurements were 100 bar and 125 °C for hydrogen absorption, and 0 bar (ca. 20 mbar) and 160 °C for hydrogen desorption.

3 Results

3.1 Compaction behaviour

Several compacts were prepared according to the procedure explained in the previous section. After manufacture, the apparent density of each compact was determined by measuring their mass (mg precision scale) and calculating their volumes (as cylindrical forms) from their diameter and their thickness (10^{-2} mm precision calliper). The mass of the 4-mm and 8-mm compacts was around 50 mg and 400 mg, respectively. Fig. 1 presents the values of the apparent density of several manufactured

compacts as a function of the applied compaction pressure. The surface of the compacts after preparation and prior to sorption experiments was smooth and even shiny.

A simple test was done to evaluate the pyrophoric behaviour of the compacts in comparison to the material as loose powder. First, unconsolidated non-cycled sodium alanate powder (ca. 30 mg) and non-cycled 4-mm compacts were exposed to air. As second test, non-cycled unconsolidated powder and non-cycled compacts were put in contact with water. These tests were carried-out three times, showing the same results. While unconsolidated sodium alanate powder was found to be readily pyrophoric when exposed to air (lot of sparks were observed), non-cycled compacts did not react at all. In the test with water, the non-cycled compacts do react but in a quite and calm manner, in contrast to the strong and agitated reaction of the unconsolidated powder.

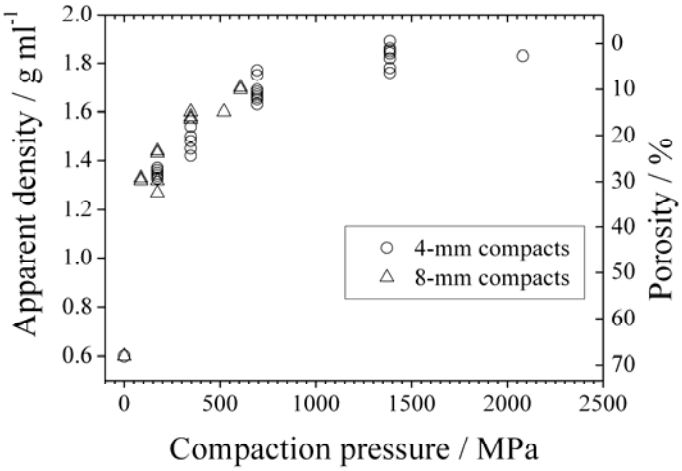

Figure 1: Apparent density and porosity of 4-mm and 8-mm compacts of sodium alanate material (desorbed state)

3.2 Sorption kinetics

Fig. 2 and 3 summarize the hydrogen sorption behaviour of consolidated sodium alanate material having different initial apparent densities. One set of compacts was prepared to a still rather low density of 1.3 g ml^{-1}, under a compaction pressure of 200 MPa. The second set was compacted to high density, 1.65 g ml^{-1}, under 700 MPa. Each set consisted of three 4-mm compacts and three 8-mm compacts. Fig. 2 shows that the hydrogen absorption of the low density compacts proceeds faster during the first three measurements in comparison to the absorption of the high density compacts. Interestingly, the high density compacts at the fifth absorption react as fast as the low density compacts after the third absorption. Similar results are found in the hydrogen desorption measurements, Fig. 3. After the second desorption, the low density compacts already present fast

kinetics. The second desorption of the high density compacts is still sluggish, but after the third desorption the kinetics is as fast as the second desorption of the low density compacts. The desorption kinetics seems to maintain the same profile in the subsequent desorption measurements. In addition, the total hydrogen capacity of both sets of compacts is surprisingly higher than 4.5 wt%. This value is higher than the total capacity observed during hydrogenation of loose powder (3.9 wt% [19]) and even close to the theoretical capacity of the material (5.0 wt% when inert material is taken into account). After a total of 12 absorption/desorption cycles, the hydrogen capacity of the compacts remains at 4.5 wt%. In addition, the compacts retained a stable structure and form (no disintegration was noticed).

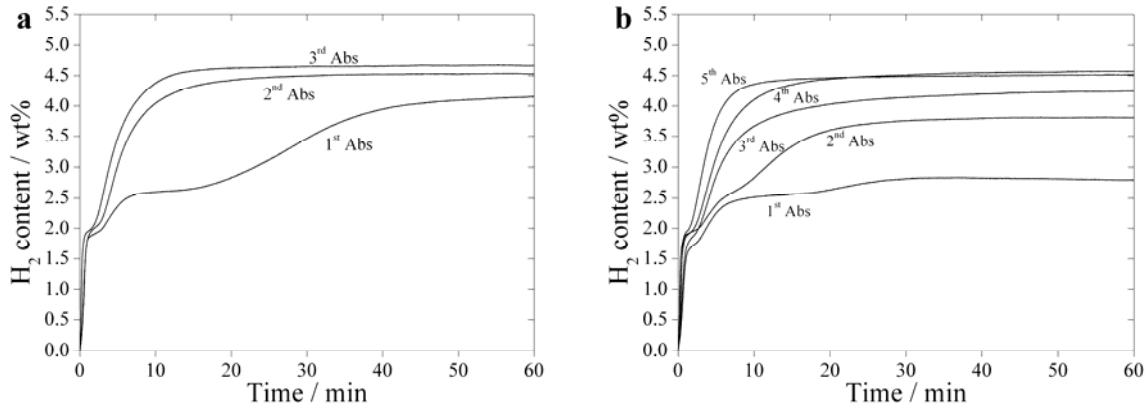

Figure 2: Absorptions of sodium alanate compacts at 100 bar and 125 °C. (a) Compacts of initial low density (1.3 g ml^{-1}). (b) Compacts of initial high density (1.6 g ml^{-1}).

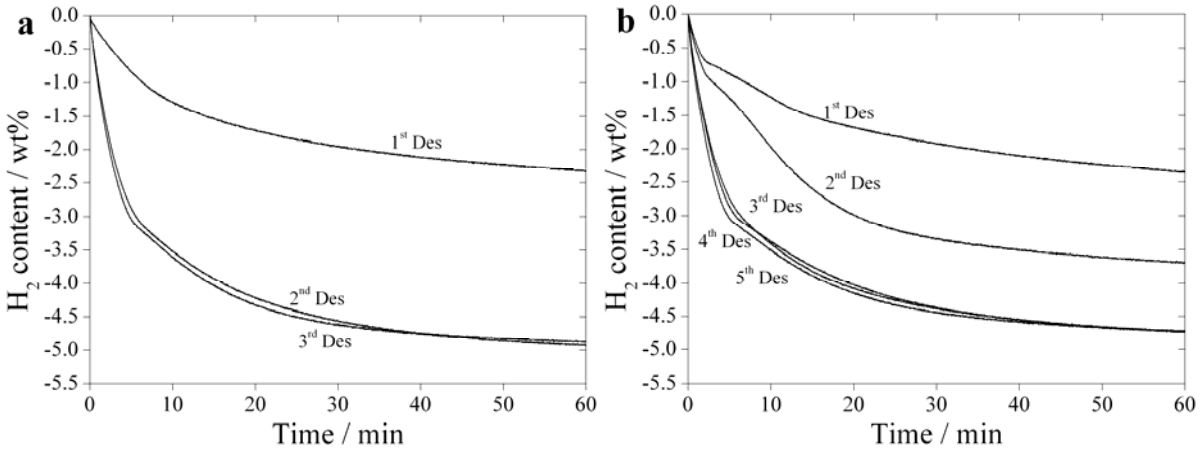

Figure 3: Desorptions of sodium alanate compacts at 0 bar and 160 °C. (a) Compacts of initial low density (1.3 g ml^{-1}). (b) Compacts of initial high density (1.6 g ml^{-1}).

3.3 Apparent density through cycling

After each sorption shown in Fig. 2 and 3, the cell of the Sieverts' apparatus was dismounted in order to inspect the compacts and to determine their apparent density. Fig. 4 shows the apparent densities of the 4-mm and 8-mm compacts, of both initial low and high density. The apparent density in Fig. 4 corresponds to the arithmetic mean of the values of the three compacts of the same type. The apparent density measured after the preparation of the compacts is reported as the initial value. After attaching the cell with the compacts for the first time at the Sieverts' apparatus, they were put under vacuum at 160 °C for 2 hours. The apparent density after these 2 hours is reported in Fig. 4 as 0^{th} desorption. Subsequently, the apparent densities are reported as the cycling was carried out (absorption/desorption). It can be observed that the apparent density of both low and high density compacts diminishes during cycling. This decrease is caused by the dimensional expansion of the compacts. After several absorption/desorption cycles, the apparent density of both low and high density compacts tends to the same value, approx. 1 to 1.1 g ml^{-1}, which corresponds to a porosity of around 45 % (referred to the material in the desorbed state). Inspection of compacts after cycling revealed that their surface was neither smooth nor shiny, contrary to the state after preparation. Marked cracks were found on the surface of the compacts compacted to high density. Fig. 5 and 6 are SEM (scanning electron microscope) images of the surface of the compacts, both fresh manufactured and after 12 absorption/desorption cycles. When compared to the fresh manufactured state, the surface of the cycled compacts reveals a change in the structure of the compact as cracks and channels can be observed.

The simple test to evaluate the pyrophoric behaviour was likewise performed to high and low density compacts after the cycling, showing to be safer in comparison to loose powder as well. When exposed to air, the cycled low-density compacts did not present pyrophoric character. A temperature increase was anyway noticed after the air exposure. On the other hand, the cycled high density compacts, although did not react with air immediately, released sparks after some manipulation followed by self-ignition. In the water test, similarly to non-cycled compacts, both the cycled high and low density compacts do react strongly but in a quite and calm manner (effervescent reaction).

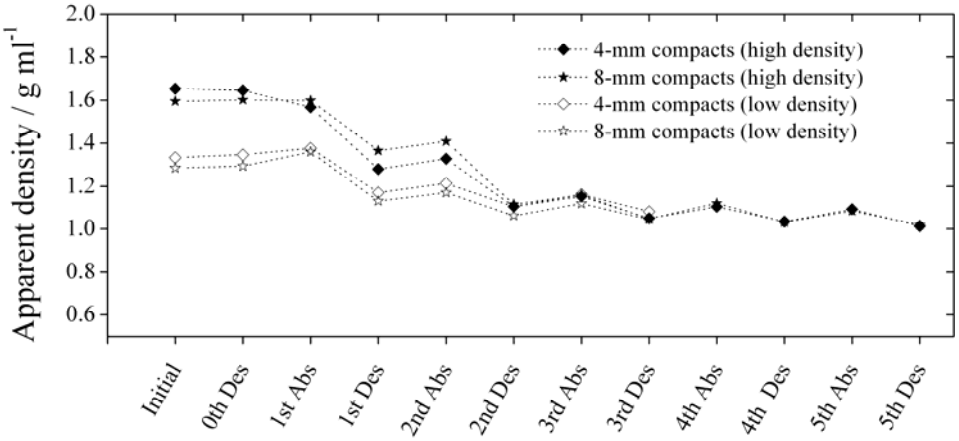

Figure 4: Apparent densities of compacts after hydrogen absorptions and desorptions. Compacts were manufactured to low density (1.3 g ml^{-1}) and high density (1.6 g ml^{-1}).

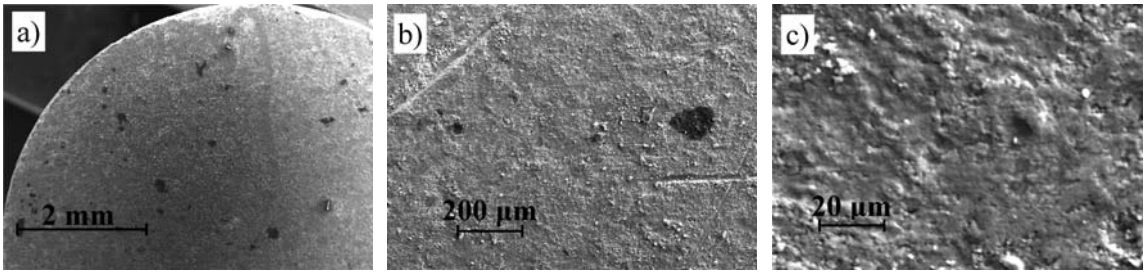

Figure 5: SEM images of the surface of a fresh manufactured 8-mm compact of sodium alanate material. Compaction pressure 200 MPa, initial apparent density 1.3 g ml^{-1}. a) Magnification 20×. b) Magnification 200×. c) Magnification 1000×.

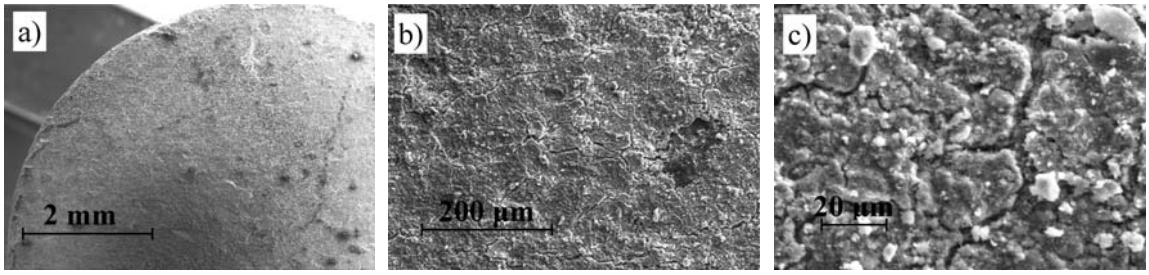

Figure 6: SEM images of the surface a 8-mm compact of sodium alanate material after 12 absorption/desorption cycles (absorbed state). Compaction pressure 200 MPa, final apparent density 1.1 g ml^{-1}. a) Magnification 20×. b) Magnification 200×. c) Magnification 1000×.

4 Discussion

Fig. 1 shows that after consolidation under different pressures, the apparent density of sodium alanate material compacts can be increased from 0.6 g ml^{-1} to over 1.8 g ml^{-1}. Thus, consolidation can triplicate the effective volumetric hydrogen storage density of the desorbed material. Powder compaction promotes a better packing of the solid particles by rearrangement and further deformation of the particles [22], such that the void interparticulate volume decreases and thus the porosity. It is clearly seen, that the applied compaction pressure has an effect on the apparent density of the compacts. Moreover, according to the results shown in Fig. 1 this effect is independent of the size of the compact (see apparent density of the 4-mm and 8-mm compacts). Under pressures from 0 MPa up to 700 MPa, the apparent density increases rapidly. At compaction pressures greater than 1400 MPa, the apparent density further increases although slower, asymptotically tending to the theoretical density of the material in the desorbed state (1.88 g ml^{-1}).

The enhancement of sorption kinetics and hydrogen capacity by cycling the low and high density compacts, shown in Figs. 2 and 3, is explained by changes of the internal packing arrangement and expansion of the compacts, as well as the increase of the solid/gas interface area (microstructural changes). This is reflected in the evolution of the apparent density of the compacts, Fig. 4, and on the SEM images of Fig. 5 and 6. First, it is noted that just the first heating up to 160 °C does not change the apparent density of the compacts. Later, it could be expected that the first hydrogen absorption of the material would decrease the apparent density from around 1.8 g ml^{-1} to a value lower than the theoretical density of $NaAlH_4$, 1.2 g ml^{-1}. The material actually does not fully react. The low porosity of the compact may have had an associated low permeability for hydrogen flow, which caused the lower hydrogen uptake obtained and that the apparent density stayed over 1.2 g ml^{-1}. After some cycles the apparent density diminishes and the porosity increases: hydrogen reacts with the compacts during absorption and is released during desorption, expanding and fracturing the compact (see Fig.

6), creating thereby new pathways for the hydrogen flow and thus increasing the permeability and particle interfaces. It resulted in higher hydrogen uptake and faster kinetics. This effect occurs in earlier cycles in the low density compacts, since they started with higher porosities than the high density ones. In both cases the apparent density tends to the same value (approx. 1 to 1.1 g ml^{-1}), indicating that the final particle arrangement in the compacts could be quite similar. Nevertheless, the higher expansion of the high density compacts caused fragmentation, which may be an undesired effect if steady shape and integrity of the compacts is desired.

Interestingly, it is during hydrogen desorption when the compact expansion is markedly observed. In order to show this in a clear manner, the dimensional change of the compacts through cycling is shown in Fig. 7. Inspection of the volume change after the first desorption in comparison to the volume after the first absorption, reveals that during desorption the compacts expand the most. For instance, in Fig. 7b (8-mm high density compacts) the largest change of volume occurs after the first desorption (+16 %) and after the second desorption (+26 %). In contrast, the expansion during absorptions is less and the compact rather slightly shrinks (on average -1.6 %). These observations may be explained by tensile stresses during hydrogen desorption promoting crack formation and fragmentation by which the particle arrangement in the compact expands. This effect is higher than the contraction of the volume of the solid phase inside the compact: the density of the solid phase increases from the absorbed state ($NaAlH_4$: ca. 1.2 g ml) to the intermediate state (Na_3AlH_6+Al: ca. 1.5 g ml^{-1}), and increases even further when transformed into the complete desorbed state (NaH+Al: ca. 1.8 g ml^{-1}). It is well known that hydrogen desorption can be used to foam metals (e.g. aluminium and zinc alloys), in which small amounts of metal hydrides (e.g. TiH_2, MgH_2) are mixed with metal powders and afterwards compacted [23]. It is found that when the melting point of the metal is far above than the desorption temperature of the metal hydride, the compact expands in the solid state during hydrogen desorption, yielding crack-like pores [23]. This is the case during sodium alanate desorption. In the case of hydrogen absorption, compressive stress occurs and leads to smaller crack and pore volume fraction in the compact, resulting into the shrinkage of the compact.

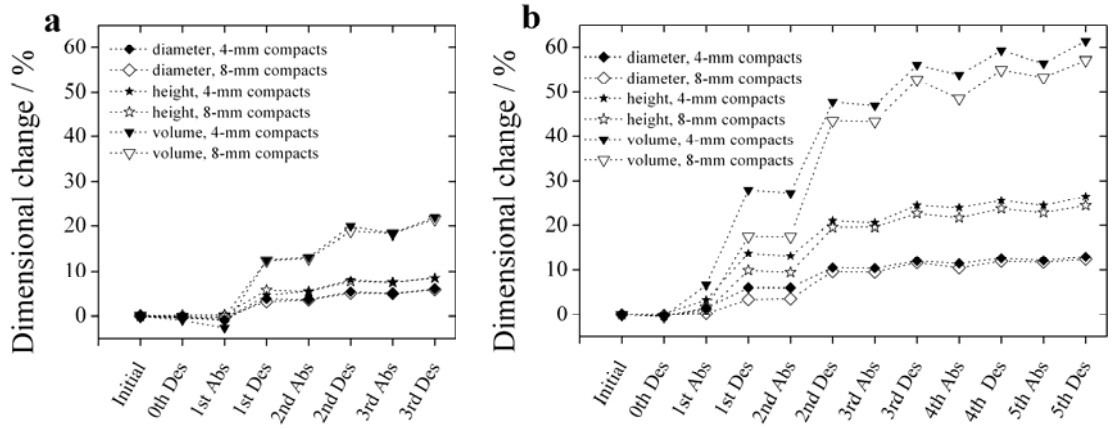

Figure 7: Dimensional change of diameter, height and volume of the compacts after different sorptions. (a) Compacts of initial low density (1.3 g ml^{-1}). (b) Compacts of initial high density (1.6 g ml^{-1}).

Compaction of the powder brings advantages for the storage capacity and safety. Higher hydrogen uptake by the compacts is obtained in comparison to unconsolidated powder. This may be due to narrower diffusion pathways for the solid reaction and the lower tendency to phase segregation in the compact. Compacts also proved to be safer to handle in contact with air and water compared to the unconsolidated power. The diminished porosity and thus less surface area and lower permeability impede or slow the pyrophoric reaction with air and the strong and agitated reaction with water. It is also to be mentioned that the prepared compacts did not disintegrate after absorption/desorption cycling. For the preparation no additional binder was added, in contrast to other metal hydride systems. This may be due to the fact that aluminium, a rather soft material, possesses a double function in the compacts: reactant (see Eq. 1 and 2) and binder. Aluminium has been proven to be an appropriated binder in the case of MgH_2 pellets [10, 12]. The presence of aluminium is a positive inherent characteristic of the sodium alanate material system, since an additional binder would decrease the weight capacity of the material.

5 Conclusions

Motivated by the potential advantages of metal hydride compaction (increased volumetric hydrogen capacity and thermal conductivity as well as easier manipulation), compacts of sodium alanate were prepared and their hydrogen sorption properties evaluated. It is demonstrated that the prepared compacts maintain its integrity after cycling and that hydrogen absorption and desorption kinetics can proceed fast. Nevertheless, there is an associated volumetric contraction/expansion of the compacts

during the first hydrogen absorption/desorption processes. These dimensional changes of the compacts must be considered when determining the internal storage cavity for the compacts. If not additional space is considered, stress of the compact against the wall may be produced which could deform or damage the container. In this sense, the information of the dimensional change can guide the dimensional design of the system. Carefully handled, the radial expansion could be used to reduce the heat transfer resistance to the wall, considering additionally the volume change by means of the height of the compacts. The crucial advantages give the compacts of sodium alanate material great potential for its use in practical hydrogen storage systems.

Acknowledgments

The authors appreciate the financial support of the European Community in the frame of the Integrated Project "NESSHY—Novel Efficient Solid Storage for Hydrogen" (contract SES6-CT-2005-518271) and of the Helmholtz Initiative "FuncHy—Functional Materials for Mobile Hydrogen Storage". The authors thank Mr. S. Walcker-Mayer and Mr. D. Meyer for their experimental support.

References

[1] L. Schlapbach, A. Züttel, Hydrogen-storage materials for mobile applications, Nature, 414 (2001) 353-358.

[2] N.B. Vargaftik, Handbook of physical properties of liquids and gases: pure substances and mixtures, 2nd Edition ed., Hemisphere publishing corporation, Washington, 1983.

[3] M. Ron, D. Gruen, M. Mendelsohn, I. Sheet, Preparation and properties of porous metal hydride compacts, Journal of the Less Common Metals, 74 (1980) 445-448.

[4] K.J. Kim, B. Montoya, A. Razani, K.H. Lee, Metal hydride compacts of improved thermal conductivity, Int. J. Hydrogen Energy, 26 (2001) 609-613.

[5] H. Ishikawa, K. Oguro, A. Kato, H. Suzuki, E. Ishii, Preparation and properties of hydrogen storage alloys microencapsulated by copper, Journal of the Less Common Metals, 120 (1986) 123-133.

[6] A. Rodríguez Sánchez, H.-P. Klein, M. Groll, Expanded graphite as heat transfer matrix in metal hydride beds, Int. J. Hydrogen Energy, 28 (2003) 515-527.

[7] H.-P. Klein, M. Groll, Heat transfer characteristics of expanded graphite matrices in metal hydride beds, Int. J. Hydrogen Energy, 29 (2004) 1503-1511.

[8] E. Tuscher, P. Weinzierl, O.J. Eder, Porous metal hydride compacts: Preparation, properties and use, Int. J. Hydrogen Energy, 8 (1983) 199-203.

[9] D.B. Willey, A.J. Williams, I.R. Harris, Preparation and Properties of metal matrix hydride compacts via the rotary forging compaction route, J. Alloys Compd., 253-254 (1997) 698-703.

[10] G. Capurso, F. Agresti, S.L. Russo, A. Maddalena, G. Principi, A. Cavallari, C. Guardamagna, Performance tests of a small hydrogen reactor based on Mg-Al pellets, J. Alloys Compd., doi:10.1016/j.jallcom.2010.11.104 (2010).

[11] A. Chaise, P. de Rango, P. Marty, D. Fruchart, S. Miraglia, R. Olivès, S. Garrier, Enhancement of hydrogen sorption in magnesium hydride using expanded natural graphite, Int. J. Hydrogen Energy, 34 (2009) 8589-8596.

[12] A. Khandelwal, F. Agresti, G. Capurso, S. Lo Russo, A. Maddalena, S. Gialanella, G. Principi, Pellets of MgH2-based composites as practical material for solid state hydrogen storage, Int. J. Hydrogen Energy, 35 (2010) 3565-3571.

[13] C. Pohlmann, L. Röntzsch, S. Kalinichenka, T. Hutsch, B. Kieback, Magnesium alloy-graphite composites with tailored heat conduction properties for hydrogen storage applications, Int. J. Hydrogen Energy, 35 (2010) 12829-12836.

[14] C. Pohlmann, L. Röntzsch, S. Kalinichenka, T. Hutsch, T. Weißgärber, B. Kieback, Hydrogen storage properties of compacts of melt-spun Mg90Ni10 flakes and expanded natural graphite, J. Alloys Compd., doi:10.1016/j.jallcom.2010.11.060 (2010).

[15] A. Züttel, P. Wenger, S. Rentsch, P. Sudan, P. Mauron, C. Emmenegger, LiBH4 a new hydrogen storage material, J. Power Sources, 118 (2003) 1-7.

[16] M. Dornheim, S. Doppiu, G. Barkhordarian, U. Boesenberg, T. Klassen, O. Gutfleisch, R. Bormann, Hydrogen storage in magnesium-based hydrides and hydride composites, Scripta Mater., 56 (2007) 841-846.

[17] U. Bösenberg, S. Doppiu, L. Mosegaard, G. Barkhordarian, N. Eigen, A. Borgschulte, T.R. Jensen, Y. Cerenius, O. Gutfleisch, T. Klassen, M. Dornheim, R. Bormann, Hydrogen sorption properties of MgH2-LiBH4 composites, Acta Materialia, 55 (2007) 3951-3958.

[18] B. Bogdanovic, M. Schwickardi, Ti-doped alkali metal aluminium hydrides as potential novel reversible hydrogen storage materials, J. Alloys Compd., 253-254 (1997) 1-9.

[19] G.A. Lozano, C. Na Ranong, J.M. Bellosta von Colbe, R. Bormann, G. Fieg, J. Hapke, M. Dornheim, Empirical kinetic model of sodium alanate reacting system (I). Hydrogen absorption, Int. J. Hydrogen Energy, 35 (2010) 6763-6772.

[20] N. Eigen, C. Keller, M. Dornheim, T. Klassen, R. Bormann, Industrial production of light metal hydrides for hydrogen storage, Scripta Mater., 56 (2007) 847-851.

[21] R. Schulz, J. Huot, S. Boily, in, 1999.

[22] R.M. German, Powder metallurgy science, Metal powder industries federation, Princeton, 1984.

[23] F. von Zeppelin, M. Hirscher, H. Stanzick, J. Banhart, Desorption of hydrogen from blowing agents used for foaming metals, Composites Science and Technology, 63 (2003) 2293-2300.

Figures Captions

Fig. 1. Apparent density and porosity of 4-mm and 8-mm compacts of sodium alanate material (desorbed state).

Fig. 2. Absorptions of sodium alanate compacts at 100 bar and 125 °C. (a) Compacts of initial low density (1.3 g ml^{-1}). (b) Compacts of initial high density (1.6 g ml^{-1}).

Fig. 3. Desorptions of sodium alanate compacts at 0 bar and 160 °C. (a) Compacts of initial low density (1.3 g ml^{-1}). (b) Compacts of initial high density (1.6 g ml^{-1}).

Fig. 4. Apparent densities of compacts after hydrogen absorptions and desorptions. Compacts were manufactured to low density (1.3 g ml^{-1}) and high density (1.6 g ml^{-1}).

Fig. 5. SEM images of the surface of a fresh manufactured 8-mm compact of sodium alanate material. Compaction pressure 200 MPa, initial apparent density 1.3 g ml^{-1}. a) Magnification 20×. b) Magnification 200×. c) Magnification 1000×.

Fig. 6. SEM images of the surface a 8-mm compact of sodium alanate material after 12 absorption/desorption cycles (absorbed state). Compaction pressure 200 MPa, final apparent density 1.1 g ml^{-1}. a) Magnification 20×. b) Magnification 200×. c) Magnification 1000×.

Fig. 7. Dimensional change of diameter, height and volume of the compacts after different sorptions. (a) Compacts of initial low density (1.3 g ml^{-1}). (b) Compacts of initial high density (1.6 g ml^{-1}).